Open access • Posted Content • DOI:10.1101/2020.06.26.174680

Pseudomonas aeruginosa uses c-di-GMP phosphodiesterases RmcA and MorA to regulate biofilm maintenance — Source link

Stefan Katharios-Lanwermeyer, Gregory B. Whitfield, P. Lynne Howell, George A. O'Toole

Institutions: Michigan State University, Université de Montréal, Hospital for Sick Children, Dartmouth College

Published on: 27 Jun 2020 - bioRxiv (Cold Spring Harbor Laboratory)

Topics: Biofilm

Pseudomonas aeruginosa uses c-di-GMP phosphodiesterases RmcA and MorA to regulate biofilm maintenance

S.L. Katharios[1], G.B. Whitfield[2,3,4], P.L. Howell[2,3] and G.A. O'Toole[1,*]

[1]Dept. of Microbiology & Immunology, Geisel School of Medicine at Dartmouth, Hanover, NH

[2]Program in Molecular Medicine, The Hospital for Sick Children, Toronto, ON

[3]Department of Biochemistry, University of Toronto, Toronto, ON

[4]Département de Microbiologie, Infectiologie et Immunologie, Université de Montréal, Montreal, QC

*To whom correspondence should be addressed:

Rm 202 Remsen Building

66 College Street

Geisel School of Medicine at Dartmouth

Hanover, NH 03755

Phone: (603) 650-1248 (office)

FAX: (603) 650-1728

email: georgeo@Dartmouth.edu

Running Title: Regulation of biofilm maintenance

Key words: biofilm, c-di-GMP, nutrient limitation, phosphodiesterase, stringent response, Pel polysaccharide

Abstract

While the early stages of biofilm formation have been well characterized, less is known about the requirements for *Pseudomonas aeruginosa* to maintain a mature biofilm. We utilized a *P. aeruginosa*-phage interaction to find that *rmcA* and *morA*, two genes which encode for c-di-GMP-degrading phosphodiesterase (PDEs) enzymes, are important for the regulation of biofilm maintenance. Deletion of these genes initially results in an elevated biofilm phenotype characterized by increased production of c-di-GMP, Pel polysaccharide and biofilm biomass. In contrast to the wild-type strain, these mutants were unable to maintain the biofilm when exposed to carbon-limited conditions. The susceptibility to nutrient limitation, and subsequent loss of biofilm viability of these mutants, was phenotypically reproduced with a stringent response mutant (Δ*relA* Δ*spoT*), indicating that the Δ*rmcA* and Δ*morA* mutants may be unable to appropriately respond to nutrient limitation. Genetic and biochemical data indicate that RmcA and MorA physically interact with the Pel biosynthesis machinery, supporting a model whereby unregulated Pel biosynthesis contributes to the death of the Δ*rmcA* and Δ*morA* mutant strains in an established biofilm when nutrient-limited. These findings provide evidence that c-di-GMP-mediated regulation is required for mature biofilms of *P. aeruginosa* to effectively respond to changing availability of nutrients. Furthermore, the PDEs involved in biofilm maintenance are distinct from those required for establishing a biofilm, thus indicating that a wide variety of c-di-GMP metabolizing enzymes in organisms like *P. aeruginosa* likely allows for discrete control over the formation, maintenance or dispersion of biofilms.

Importance

Recent advances in our understanding of c-di-GMP signaling have provided key insights into the regulation of biofilms. Despite an improved understanding of how they initially form, the processes that facilitate the long-term maintenance of these multicellular communities remain opaque. We found that *P. aeruginosa* requires two phosphodiesterases, RmcA and MorA, to

maintain a mature biofilm and that *P. aeruginosa* biofilms lacking these PDEs succumb to nutrient limitation and die. The biofilm maintenance deficiency observed in Δ*rmcA* and Δ*morA* mutants was also found in the stringent response defective Δ*relA* Δ*spoT* strain, suggesting that a regulatory intersection between c-di-GMP signaling, EPS biosynthesis and the nutrient limitation response is important for persistent surface growth. We uncover components of an important regulatory system needed for *P. aeruginosa* to persist in nutrient-poor conditions, and provide some of the first evidence that maintaining a mature biofilm is an active process.

Introduction

Pseudomonas aeruginosa is a Gram-negative opportunistic pathogen that is found both environmentally and within clinical settings. Able to transition from planktonic lifestyles to a biofilm mode of growth, *P. aeruginosa* biofilms develop via a number of discrete steps generally defined as initial attachment, irreversible attachment, microcolony formation, maturation and dispersal (1). Flagella mediate the initial polar attachment of the cell to the surface, while pili facilitate irreversible attachment and commitment to surface growth (2, 3). Once on the surface, increased production of extracellular polysaccharide (EPS) facilitates increased surface adhesion, intercellular cohesion and provides both protection and structural integrity for mature biofilms to form (3–6).

An important element in the transition of *P. aeruginosa* from a planktonic to biofilm mode of growth is bis-(3′,5′)-cyclic dimeric guanosine monophosphate (c-di-GMP), a second messenger that coordinates the regulatory control of virulence and behaviors needed for surface growth such as motility and the production of EPS (7–10). The concentration of intracellular c-di-GMP is controlled enzymatically by c-di-GMP synthesizing diguanylate cyclases (DGCs) which contain GGDEF domains, and c-di-GMP degrading phosphodiesterases (PDEs) that harbor EAL or HD-GYP domains (8, 11). The genome of *P. aeruginosa* PA14 encodes ~40 different DGCs and

PDEs involved in the regulation of c-di-GMP (12). Despite the published record of the contributions of these different enzymes to biofilm formation and dispersion (13, 14), our understanding of how they are coordinated and integrated temporally to affect bacterial behavior remains incomplete.

Select DGCs and PDEs have been shown to be important during different phases of biofilm formation. For example, the DGC SadC and the PDE BifA both contribute to irreversible attachment and early biofilm formation (15, 16). During subsequent biofilm growth, the DGC WspR mediates biofilm maturation by increasing the production of EPS (17). Regulation of c-di-GMP also facilitates the return to the planktonic lifestyle, as evidenced by the PDEs NbdA and DipA, which are required for dispersion in response to changes in nutrients and nitric oxide levels, respectively (18, 19).

While available literature provides substantial insights into how biofilms form and disperse, our understanding of biofilm maintenance - the process by which existing biofilms regulate themselves to persist on a surface is rudimentary. Indeed, it is not even clear if maintenance of the biofilm is an active process. To date, information regarding biofilm maintenance is largely informed by proteomic analysis of biofilms at specific stages of development (20), an analysis primarily conducted using biofilms grown under nutrient-rich steady-state conditions (20), leaving open the questions of if and how the regulation of biofilms occurs during starvation. Here, we provide evidence that the PDEs RmcA and MorA are needed for the maintenance of *P. aeruginosa* biofilms - the loss of either of these PDEs results in increased EPS production and biomass in nutrient-sufficient conditions, but increased cell death and compromised biofilms during starvation.

Results

CRISPR-activated genetic background reveals role of c-di-GMP signaling in biofilm maintenance. Previously, we reported that the chromosomal integration of a 42-nucleotide sequence of DNA from the bacteriophage DMS3 into the genome of *P. aeruginosa* PA14 resulted in a CRISPR-activated genetic background. The CRISPR-activated strain that carries this 42-nucleotide sequence in the attachment (*att*) site, called *att*::DMS3$_{42}$, was reported to be biofilm-negative due to increased cell death after 24 h, a typical time point to assess biofilm formation in a standard 96 well, static biofilm assay (21). Additionally, while the *att*::DMS3$_{42}$ strain was able to form a biofilm at early time points (~6 h) it was largely biofilm-negative by 12 h, suggesting that biofilm formed but could not be maintained. These data indicated to us that *att*::DMS3$_{42}$ could serve as an effective tool to probe for functions required for biofilm maintenance, a poorly characterized aspect of the biofilm life cycle. Our goal then was to exploit the robust phenotype offered by the CRISPR-activated strain to study biofilm biology.

Due to the important role of c-di-GMP in facilitating surface growth, we hypothesized that reduced levels of this second messenger contributed to the inability of *att*::DMS3$_{42}$ to maintain a biofilm at later time points. To test this hypothesis, we employed a vector expressing the GcbC-R363E mutant protein, which codes for a DGC found in *Pseudomonas fluorescens* that has a mutation in the regulatory I-site that renders it constitutively active, thereby enhancing c-di-GMP synthesis (22). We heterologously expressed this construct in the *P. aeruginosa* PA14 WT and *att*::DMS3$_{42}$ strain backgrounds to assess whether increased c-di-GMP synthesis could rescue the biofilm deficiency observed at 12 h for the latter strain. Introduction of the *gcbC*-R363E expression plasmid into the WT strain resulted in elevated biofilm biomass over the empty vector control, consistent with the increased production of c-di-GMP (**Fig. 1A**). Consistent with our hypothesis, the expression of this constitutively-active DGC in the strain carrying the

att::DMS3$_{42}$ construct greatly reduced the biofilm defect (i.e., enhanced biofilm formation) at 12 h compared to the att::DMS3$_{42}$ strain carrying the empty vector (EV) control (**Fig. 1A**). These data suggest that the inability of the strain carrying the *att*::DMS3$_{42}$ insertion to maintain the biofilm may be the result of decreased levels of c-di-GMP.

Given that the biofilm defect of the *att*::DMS3$_{42}$ strain could be rescued by heterologously expressing a c-di-GMP-synthesizing enzyme, we reasoned that the same effect might/should be observed by mutating one or more genes encoding PDEs. To this end, we built on work from Ha *et. al*. who used the SMART algorithm to analyze the genome of *P. aeruginosa* for encoded proteins with motifs related to c-di-GMP metabolism (23, 24). This approach identified 24 candidate PDEs with either EAL domains alone (6), dual GGDEF/EAL domains (15), or HD-GYP domains (3) (**Fig. 1B**). Individual in-frame deletions for all these PDEs were constructed in the *att*::DMS3$_{42}$ background and these strains were then assayed for biofilm formation. Of all the deletions of genes coding for PDE that were constructed, only two of them, Δ*rmcA* and Δ*morA*, exhibited a significant rescue of biofilm biomass at 12 h compared to the parental *att*::DMS3$_{42}$ background (**Fig. 1C**). While both *rmcA* and *morA* encode for dual (GGDEF and EAL) domains, previous work suggests that these proteins behave predominately as PDEs (25, 26). These data suggest that the defect observed in the *att*::DMS3$_{42}$ strain can be rescued by increasing concentrations of c-di-GMP either via heterologous expression of the GcbC-R63E protein (**Fig. 1A**) or through the loss of either of the two PDEs encoded by the *rmcA* and *morA* genes (**Fig. 1C**). The observation that none of the other PDEs tested could rescue the biofilm formation defect of the *att*::DMS3$_{42}$ strain (**Fig. 1B**) suggests a specific role for these particular PDEs, a point we address below.

The Δ*rmcA* or Δ*morA* mutants are defective in the later stages of biofilm formation in a static assay. We next investigated the biofilm phenotypes of the Δ*rmcA* and Δ*morA* mutants in

a WT background (no DMS3$_{42}$-mediated CRISPR activation) using a 96-well dish static biofilm assay over a 48 h window. These mutants were able to form a biofilm similar to the WT over the first ~12 h of the assay (**Fig. 2A**). Between 12 and 24 h, while WT biofilm biomass continues to increase, the biomass of the Δ*rmcA* and Δ*morA* mutants plateau and begin to decrease, and increasingly exhibit a defect in biofilm biomass out to 48 hr. Between 24 and 48 h the WT biofilm is maintained with no obvious loss of biomass in this assay.

To assess if the behavior of Δ*rmcA* and Δ*morA* is dependent on the type of carbon source provided, we replaced the carbon source used in our standard medium, L-arginine, with pyruvate. We found that that the Δ*rmcA* and Δ*morA* mutant biofilms also exhibit a late-stage defect at 36 h in this medium, while the 12 h biofilms were similar to WT (**Fig. S1**). To verify that the loss of biofilm that we observed in late timepoints of our kinetic assay was dependent on the absence of either RmcA or MorA we complemented these mutants, and found that the late stage biofilm defect observed in these mutants could be rescued by a wild-type copy of *rmcA* and to a lesser extent for *morA*, respectively (**Fig. 2B & C**).

The Δ*rmcA* and Δ*morA* mutants have increased c-di-GMP levels. Given that RmcA and MorA are predicted PDEs (25, 26), we would expect that the Δ*rmcA* and Δ*morA* mutants would have increased levels of c-di-GMP compared to the WT strain. To test this hypothesis, we measured total c-di-GMP in the mutants versus WT using a P$_{cdrA}$-*gfp* promoter fusion to assess transcriptional activity of *cdrA,* a gene that is positively regulated by c-di-GMP (27). The GFP signal serves as a surrogate for c-di-GMP levels. We normalized the amount of GFP signal produced to a constitutively expressed orange fluorescent protein, mKO (28), integrated into the *att* chromosomal insertion site. This assay provided us with an indirect, but normalized measure of the relative c-di-GMP concentration in WT versus mutant backgrounds. Biofilms were grown in a static assay on coverslips that were partially submerged in buffered biofilm medium

containing 0.4% arginine in a 12-well dish, as described (29). The coverslips were then incubated for 24 h, similar to the static biofilm assays shown in **Figure 1** and **Figure 2**, prior to imaging of the air-liquid interface (ALI) with brightfield and fluorescence microscopy.

Mutation of either *rmcA* or *morA* resulted in an increase of P_{cdrA}-*gfp* fluorescence (**Fig. 2D**). The structures of the WT and mutant biofilms also differed, with the WT generating typical "mushroom-like" colonies, while the mutants formed a uniform layer of cells. Thus, it was important to examine the normalized signal intensity of individual cells to accurately compare the average signal intensity between strains. On a cell-by-cell basis, with values normalized to mKO signal intensity, both the Δ*rmcA* and Δ*morA* mutants exhibited a significant increase in signal intensity from the P_{cdrA}-*gfp* reporter of 3.6- and 5.0-fold over WT, respectively (**Fig. 2E**). These results are consistent with the previous reports that both *rmcA* and *morA* encode for active PDEs and that the loss of these enzymes would result in reduced degradation of c-di-GMP.

Given the observation that strain backgrounds with a late-stage biofilm deficiency also had elevated c-di-GMP, we hypothesized that this deficiency could be induced in WT or enhanced in Δ*rmcA* and Δ*morA* mutants simply by increasing c-di-GMP production. To test this hypothesis, we measured biofilm levels at several time points in WT and mutant backgrounds that were heterologously expressing *gcbC*-R363E from a plasmid. As exhibited in **Fig. S2** however, increasing c-di-GMP production alone is insufficient to induce a late-stage biofilm deficiency in the WT, nor is it capable of accelerating the kinetics of the observed biofilm defect in the Δ*rmcA* and Δ*morA* mutant backgrounds. These data suggest that the observed phenotypes are linked to the loss of *rmcA* and *morA* specifically, rather than to a general increase in c-di-GMP levels.

The inability of Δ*rmcA* and Δ*morA* to maintain a late-stage biofilm is correlated to nutrient limitation. The death observed in late stage biofilms in the static assay indicated that perhaps, as nutrients become limited in this batch culture, the Δ*rmcA* and Δ*morA* mutants were unable to adapt to these nutrient-limited conditions and thus exhibited reduced viability. We tested this hypothesis in two ways. First, we conducted static 96-well biofilm assays in which biofilm formation was measured early (12 h) and late (48 h), and then compared these results to biofilms grown for the same 48 h, but with periodic (every 12 h) removal of spent medium followed by the addition of fresh medium. That is, periodic replacement of the medium provided cells with regular access to fresh nutrients even in the batch culture system. We found that, compared to late timepoints in the standard assay (no medium replacement) wherein the Δ*rmcA* and Δ*morA* mutants exhibited a biofilm defect (55.7% and 82.5% reduction, respectively; **Fig. S3A**), the removal and replacement of spent medium with fresh medium results in the reduction of the magnitude of this defect to an 11.6% reduction in Δ*rmcA* and an 33.1% reduction in Δ*morA* (**Fig. S3B**), levels comparable to that observed for an early stage biofilm formed by the Δ*morA* mutant at 12 h (**Fig. S3C**).

We next assessed whether oxidative stress could result in a similar cell death phenotype. We grew biofilms for 12 h in a static 96 well assay, a time point wherein we have detected minimal evidence of starvation responses within the biofilm (**Fig. 2A and S4A**). We next replaced the spent medium with fresh medium supplemented either with 20 mM H_2O_2 (**Fig. S4B**) or no H_2O_2 (**Fig. S4C**) and then incubated the biofilms for an additional 6 h. The addition of H_2O_2 had no impact on the WT or mutant biofilms (**Fig. S4B**) compared to the control (**Fig. S4C**). Taken together, these results are consistent with the hypothesis that the defect that we observe in the Δ*rmcA* and Δ*morA* mutants is due to an inability to appropriately respond to nutrient limitation, rather than a general stress response.

The inability of the Δ*rmcA* and Δ*morA* mutants to maintain biofilm correlates with increased cell death. To explain the loss of late-stage biofilms in the Δ*rmcA* and Δ*morA* mutants we tested the hypothesis that these mutants were dying, thereby causing the loss of biofilm biomass. We imaged biofilms after staining with the LIVE/DEAD *Bac*Light kit (Molecular Probes). This assay allowed us to determine the ratio of cells that are viable (i.e., those stained green by membrane-permeable Syto9) to those that are dead (i.e., cells with compromised membranes that are stained red by membrane-impermeable propidium iodide). Biofilms were stained with *Bac*Light after 16 h or 48 h of static growth in the ALI assay in 12 well plates, as described above, and the data plotted as the ratio of live cells (green) to dead cells (red).

After 16h, biofilms of all strain backgrounds were comprised of predominantly viable cells (**Fig. 3A**, top row) with the Δ*morA* mutant displaying a live/dead ratio similar to WT, while the Δ*rmcA* mutant live/dead ratio was significantly higher than the WT even at this early time point (**Fig. 3B,** left panel). After 48 h in the static assay, however, the Δ*rmcA* and Δ*morA* mutants were significantly less viable than WT (**Fig. 3A**, bottom row) with the live/dead ratios of Δ*rmcA* and Δ*morA* mutants reduced by 55.7% and 43.3%, respectively (**Fig. 3B,** right panel)**.** While both mutants exhibited a reduced ratio of live/dead cells, individual comparisons of Syto9 and PI (**Fig. S5A and B,** respectively) reveal that the reduction observed in Δ*rmcA* mutant is driven both by an increase in the number of dead cells and a decrease in live cells, whereas while in Δ*morA* mutant the change in this ratio reflects primarily the loss of viable (green) cells. The inability to detect a significant increase in dead cells within late-stage Δ*morA* biofilm could be due to an earlier onset of death followed by the sloughing off of dead cells prior to microscopy at 48 h, a conclusion consistent with the findings presented below.

To address whether we could recapitulate the impact of nutrient-limited conditions observed in our static assays, we utilized a microfluidic device that allowed us to observe biofilm dynamics

in real time and to manipulate the amount of nutrients provided. We first confirmed that all three strains could form biofilm within a microfluidic chamber. To monitor biofilm formation, we introduced the pSMC21 plasmid, which constitutively expresses GFP (30, 31), into each of the strains. The bacteria were inoculated into the microfluidic chamber, allowed to attach for 1 h prior to the start of flow (0.5 µl/min), then monitored at 45 min intervals using fluorescence microscopy over the first 12 h of biofilm formation. The Δ*rmcA* and Δ*morA* mutants are able to form robust biofilms in the microfluidic chamber (**Fig. S6**).

We hypothesized that we could recapitulate in a microfluidic chamber the nutrient-limited conditions that developed over late timepoints in the static assays by establishing the biofilms in a medium that contained a carbon source, then irrigating the biofilms with medium lacking a carbon source. To test this idea, we allowed biofilms of the WT and mutants carrying the GFP-expressing plasmid pSMC21 to form a biofilm for 24 h in biofilm medium with arginine as the carbon source, then switched to biofilm medium lacking arginine. One hour before the switch to nutrient-limited conditions, we stained the microfluidic chamber-grown biofilms with PI to label non-viable cells and thus establish a baseline of non-viable cells before inducing nutrient limitation. As shown in **Figure 3C** and **Figure 3E**, at time zero before nutrient limitation is induced, all three strains formed a robust biofilm and showed minimal non-viable cells.

To assess if nutrient limitation differentially impacted loss of biofilm in the WT compared to the mutants, we normalized the GFP signal to the start of nutrient limitation for each strain (t = 0 in **Fig. 3C**, top), then recorded the change in GFP intensity over the subsequent 36 h of exposure to carbon-free medium. While WT was largely able to maintain the biofilm over the course of the assay, the lack of carbon in the growth medium accelerated the loss of biomass in both the Δ*rmcA* and Δ*morA* mutant biofilms. This was evidenced by the greater reduction of the GFP-mediated signal intensity in the mutants compared to the WT during the 36 h period of carbon

limitation (**Fig. 3C-D**). The WT lost ~25% of biomass compared to a >50% reduction for both the Δ*rmcA* and Δ*morA* mutants over the 36 h of the experiment.

To assess if these mutants lost biofilm biomass over the course of nutrient limitation due to increased death, as observed in the static assay in **Figure 3A**, we measured the intensity of PI over time and found that both the Δ*rmcA* and Δ*morA* mutants exhibited rapidly increasing PI staining in absolute terms (**Fig. 3E**) and as a ratio of GFP fluorescent intensity, which served as a measure of total biofilm biomass of viable cells (**Fig. 3F**). These data provide further evidence that both the Δ*rmcA* and Δ*morA* mutants are susceptible to nutrient-limited conditions when grown in a biofilm, and that loss of late-stage biofilm biomass coincides with cell death.

To determine if dispersal of the biofilm could contribute to the observed loss of biofilm biomass upon nutrient limitation, we measured the viable count (CFU) of bacteria dispersing from biofilms within a microfluidic device prior to and after nutrient limitation. As shown in **Figure S7**, effluent-derived cells of all strains were similar 2 h prior to, as well 12 and 18 h after, the switch to arginine-free medium. Only in the final timepoint (24 h) did the viable count of the Δ*rmcA* and Δ*morA* effluent increase compared to WT. These data suggest that cell death, and not dispersal, is the primary driver of the loss of biomass observed in these PDE mutants during nutrient limitation.

A stringent response mutant phenocopies the biofilm cell death of Δ*rmcA* and Δ*morA* mutants during nutrient limitation. The ability of the Δ*rmcA* and Δ*morA* mutants to maintain a biofilm when nutrients were present coupled with the decrease in viability during nutrient limitation suggested that these mutants were unable to mediate the appropriate responses needed for persistence when resources become limiting. This conclusion was further supported by the observation that the biofilm defect in the static assay for the Δ*rmcA* and Δ*morA* mutants

could be rescued simply by adding fresh medium (**Fig. S3**). Based on these data, we hypothesized that loss of RmcA or MorA function results in the inability to appropriately navigate nutrient limited conditions.

If this hypothesis is correct, other strains defective in the nutrient limitation-response should have a similar phenotype. To test this prediction, we assessed the phenotype of a Δ*relA* Δ*spoT* double mutant, which is unable to either make or degrade the alarmone (p)ppGpp critical for the stringent response, for its ability to respond to nutrient limitation when grown in a biofilm. We first assessed biofilm formation of the Δ*relA* Δ*spoT* mutant in static assays and found that, like the Δ*rmcA* and Δ*morA* mutants (**Fig. 2A**), the Δ*relA* Δ*spoT* mutant could form a biofilm (albeit at a level lower than the WT) at early time points and biofilm biomass was reduced at later time points (**Fig. 4A**).

Next we used a microfluidic chamber where nutrient-limited conditions could be induced via introduction of carbon-free medium. Using the same conditions we used above (**Fig. 3**), we found that for the Δ*relA* Δ*spoT* mutant, which is unable to mount a stringent response, the loss of biofilm biomass (**Fig. 4B**) and viability (**Fig. 4C-D**) occurs concurrently with nutrient limitation.

Loss of RmcA and MorA function is associated with increased Pel polysaccharide production in the biofilm. Increased c-di-GMP is typically associated with enhanced biofilm formation. To reconcile how mutants that have a late-stage biofilm defect (**Fig. 3**) also produce increased c-di-GMP (**Fig. 2C-D**), we hypothesized that the loss of biofilm observed in the Δ*rmcA* and Δ*morA* mutants was the result of untimely cellular investment in energetically expensive products. Such a view is consistent with the kinetics of the defect observed for the Δ*rmcA* and Δ*morA* mutants, which becomes increasingly evident after ~30 h of growth in static conditions,

335 when nutrients are likely depleted, and after a shift to carbon-free medium in the microfluidic
336 device.
337
338 To evaluate whether the increased concentration of c-di-GMP in late-stage biofilms also
339 resulted in altered phenotypes relevant to biofilm formation, we assessed production of
340 extracellular polysaccharide (EPS) in the WT and the Δ*rmcA* and Δ*morA* mutants. In *P.*
341 *aeruginosa* PA14 the dinucleotide c-di-GMP up-regulates Pel production. Both mutants showed
342 enhanced pellicle production compared to the WT, with accumulated biomass on the tubes of
343 overnight-grown planktonic cultures (**Fig. 5A**). We also employed Congo Red (CR), a dye which
344 can be used as a qualitative indicator of the presence of EPS, combined with colony biofilm
345 assays on agar medium. The Δ*rmcA* and Δ*morA* mutants showed enhanced CR binding after 4-
346 5 days compared to the WT (**Fig. 5B**), consistent with the view that the loss of RmcA and MorA
347 results in increased c-di-GMP and EPS production.
348
349 To test if the Pel polysaccharide specifically was being overproduced in the Δ*rmcA* and Δ*morA*
350 mutants, we used fluorescein-labelled *Wisteria floribunda* lectin (WFL) which binds preferentially
351 to carbohydrate structures that terminate in *N*-acetylgalactosamine. This lectin has been shown
352 to bind specifically to the Pel polysaccharide (32). WFL was used to stain statically grown ALI
353 biofilms and the fluorescent signal was normalized to a constitutively expressed fluorescent tag,
354 mKO, as described above. Biofilms of the Δ*rmcA* and Δ*morA* mutants demonstrated elevated
355 WFL binding (**Fig. 5C**), with signals from the Δ*rmcA* and Δ*morA* mutants significantly increased
356 by 2.8- and 1.9-fold above WT, respectively (**Fig. 5D**). Combined, these data suggest that both
357 the Δ*rmcA* and Δ*morA* mutants produce increased levels of the Pel EPS when growing as a
358 biofilm, consistent with the elevated levels of c-di-GMP observed in these mutants (**Fig. 2**).
359

To further probe whether high levels of Pel expression in the Δ*rmcA* and Δ*morA* mutants was necessary and/or sufficient to induce late cell death. First, we introduced a Δ*pelA* mutation into the Δ*rmcA* and Δ*morA* backgrounds, but unfortunately, the Δ*rmcA* Δ*pelA* and Δ*morA* Δ*pelA* double mutants were defective for establishing a biofilm (**Fig. S8A**), which is expected given the role of Pel in biofilm formation (40), so we could not perform the desired analyses in these strains. Instead, we used a strain that allowed us to artificially induce Pel expression to high levels – this strain did not show enhanced death in late stage biofilms (**Fig. S8B**). This second observation indicates that while Pel production may contribute to late stage cell death in the Δ*rmcA* and Δ*morA* mutants, it is not sufficient to drive this phenotype. That is, the high levels of c-di-GMP in the Δ*rmcA* and Δ*morA* mutants may have additional negative impacts on the cell in the context of a nutritionally limited, mature biofilm.

RmcA and MorA physically interact with PelD. The data presented thus far suggests that appropriate Pel regulation is lost when cells lack RmcA or MorA function. The biosynthesis of Pel is regulated at the transcriptional and post-translational levels by the c-di-GMP-binding effector proteins FleQ and PelD, respectively (33, 34). DGCs and PDEs can influence the activation state of effector proteins through the alteration of global intracellular c-di-GMP pools or via specific interaction with effectors via local signaling events (35). RmcA, MorA, and PelD localize to the inner membrane due to the presence of one or more predicted transmembrane helices (25, 36, 37), therefore we hypothesized that RmcA and/or MorA may influence Pel biosynthesis through direct interactions with PelD.

To assess possible RmcA/MorA/PelD interactions, a vesicular stomatitis virus glycoprotein (VSV-G)-tag was added to the C-terminus of RmcA and MorA (RmcA-V and MorA-V), and the genes expressing these tagged proteins were integrated at the neutral chromosomal *att*::Tn*7* site under the control of the *araC*-P_{BAD} promoter in *P. aeruginosa* strains lacking a native copy

386 of the *rmcA* or *morA* genes, respectively. To ensure that the activity of RmcA or MorA did not
387 influence the c-di-GMP-dependent transcription of the *pel* operon by FleQ, the Pel
388 overproducing strain *P. aeruginosa* PAO1 Δ*wspF* Δ*psl* P_{BAD}*pel* was utilized (38). Co-
389 immunoprecipitation (co-IP) was performed from solubilized, enriched inner membranes of *P.*
390 *aeruginosa* overexpressing the RmcA-V or MorA-V tagged proteins and the protein components
391 encoded by the *pel* operon by the addition of L-arabinose to culture media. In each experiment,
392 PelD was detected in the eluate via Western blot when RmcA-V or MorA-V were supplied as the
393 bait, but not in the untagged control eluate (**Fig. 5E**). These data suggest that RmcA and MorA
394 may interact with PelD to exert their control over Pel biosynthesis.
395
396 While the data gathered by co-IP suggests an interaction between RmcA/MorA and PelD, it
397 does not distinguish between direct interactions or those mediated by other unknown proteins.
398 To validate these findings using a different approach, interactions between RmcA/MorA and
399 PelD were analyzed using bacterial two hybrid (BACTH) assays. In these experiments, the
400 inactive T18 fragment of *Bordetella pertussis* adenylate cyclase toxin was fused to the N-
401 terminus of RmcA or MorA (T18-RmcA or T18-MorA), while the inactive T25 adenylate cyclase
402 fragment was fused to the N-terminus of PelD (T25-PelD). Interaction between T18-RmcA/T18-
403 MorA and T25-PelD would reconstitute adenylate cyclase enzymatic activity, and lead to the
404 production of blue colonies when analyzed in the *E. coli* BTH101 reporter strain grown on agar
405 medium containing X-Gal.
406
407 When interactions between T18-RmcA and T25-PelD were examined in the BACTH assay,
408 white colonies were observed, indicative of a negative result (**Fig. 5F**). Since interactions
409 between RmcA and PelD were identified by co-IP in a *P. aeruginosa* background where the
410 entire *pel* operon was overexpressed (**Fig. 5E**), and PelD directly interacts with both PelE and
411 PelG to form the inner membrane Pel synthase complex regardless of its c-di-GMP binding

412 capability (36), we reasoned that expressing untagged PelE, PelG, or both co-polymerase
413 proteins alongside T18-RmcA and T25-PelD would better imitate the physiological conditions
414 under which this interaction is presumed to occur. When these modified BACTH experiments
415 were performed, we observed bright blue colonies comparable to the positive control when both
416 PelE and PelG were co-expressed with T18-RmcA and T25-PelD, but only very faint blue to
417 white colonies when PelE or PelG were singly co-expressed (**Fig. 5F**). Similar results were
418 obtained when the modified BACTH experiment was performed with T18-MorA and T25-PelD,
419 where a deep blue colony indicative of a positive result was observed when both untagged PelE
420 and PelG were co-expressed (**Fig. 5G**). However, unlike with RmcA, a weak-to-moderate
421 positive result was also obtained when only untagged PelE, untagged PelG, or even an empty
422 vector control was present (**Fig. 5G**). These data collectively show that both RmcA and MorA
423 physically interact with PelD, but do so maximally under conditions where other components of
424 the Pel synthase complex are present alongside PelD (39), as illustrated in **Figure 5H**.
425
426
427 **Discussion**
428
429 Exploiting previous findings from our lab in which a CRISPR-activated strain exhibited a defect
430 in biofilm maintenance (21), we discovered that two PDEs, RmcA and MorA, were essential for
431 maintaining late-stage biofilms. The Δ*rmcA* and Δ*morA* mutants exhibit phenotypes consistent
432 with the inability to degrade c-di-GMP, specifically, elevated c-di-GMP, increased Pel production
433 and the ability to initiate a robust biofilm. Yet, the Δ*rmcA* and Δ*morA* mutants fail to maintain the
434 biofilm in long term static assays or when established biofilms are deprived of a carbon source
435 in a microfluidic chamber. Additionally, we have shown that the inability to maintain biofilms in
436 these mutant backgrounds is driven by widespread cell death during nutrient limitation.
437 Consistent with the hypothesis that cell death in these mutants is due to an aberrant nutrient

limitation response, we showed that the Δ*relA* Δ*spoT* mutant, which lacks the ability to induce a stringent response, demonstrates a biofilm maintenance defect during nutrient limitation similar to that observed for the Δ*rmcA* and Δ*morA* mutants.

Taken together, the above data suggests a model (**Fig. 6**) whereby the production of the energetically expensive Pel polysaccharide, required for the initial steps of biofilm formation, is downregulated by RmcA and MorA during biofilm maintenance when nutrient limitation conditions predominate. As such, while the loss of either PDE results in increased EPS and enhanced biofilm growth, a boon to these microorganisms in resource-rich environments typical of early biofilm formation, it leaves the cells unable to adapt to later nutrient-limited conditions in the context of a mature biofilm.

The mechanisms by which RmcA and MorA are regulated in nutrient-limited conditions remain unknown, however recent findings within *Pseudomonas putida* provide a potential signaling framework. Work by Carlos Díaz-Salazar et al. found that RelA and SpoT-dependent synthesis of (p)ppGpp mediates dispersal during nutrient-limited conditions (40). This group also found that (p)ppGpp increased transcription of the PDE *bifA* and that a Δ*bifA* mutant was defective in starvation-induced biofilm dispersal (40, 41). It is possible that RmcA and MorA within *P. aeruginosa* operate analogously to that of BifA in *P. putida* by acting as effectors of stringent response signaling during nutrient-limited conditions. Unlike BifA in *P. putida*, RmcA and MorA do not coordinate dispersal in *P. aeruginosa*, but rather participate in effectively maintaining the biofilm in the face of nutrient limitation.

The high levels of c-di-GMP in the Δ*rmcA* and Δ*morA* mutants may have adverse impacts on the cells in nutritionally-limited, mature biofilms. While we do not yet completely understand how the regulation of Pel may contribute to biofilm maintenance, there is strong evidence for the

464 physical interaction of RmcA and MorA with PelD and other elements of the Pel biosynthetic
465 machinery (**Fig. 5E-H**), suggesting that RmcA and MorA may have a direct role in regulating
466 Pel synthesis. However, as noted above, artificially increasing Pel expression to high levels
467 does not result in increased cell death in nutrient-limited condition (**Fig. S7B**), suggesting that
468 the overexpression of Pel alone is insufficient to drive the late-stage cell death phenotype of the
469 Δ*rmcA* and Δ*morA* mutants.
470
471 Further studies are needed to elucidate whether the potential role of Pel in biofilm maintenance
472 is related to the stringent response. It is possible that the inability to appropriately regulate c-di-
473 GMP and EPS production during nutrient limitation impacts (p)ppGpp levels, eventually resulting
474 in extensive cell death and biofilm degradation. Alternatively, the ability to induce a stringent
475 response may be part of a coordinated down-regulation of metabolic activity required for the
476 long-term maintenance of a mature biofilm, particularly when carbon/energy sources are
477 limiting. Additionally, Pseudomonads appear to have developed catabolic pathways for the
478 utilization of arginine and lactate for “maintenance energy” in mature biofilms (43, 44), as well
479 as a pathway to down-regulate flagellar motility, another early-stage biofilm factor, in mature
480 biofilms (1). Taken together, these data indicate that Pseudomonads, and likely other microbes,
481 have active, well-regulated mechanisms necessary to maintain a mature biofilm in the face of
482 changing environmental conditions.
483
484 Finally, the apparent role for c-di-GMP-metabolizing enzymes RmcA and MorA later in the
485 biofilm lifestyle suggests the interesting possibility that the plethora of these enzymes in
486 Pseudomonads stems from their roles in regulating discrete aspects of the biofilm lifestyle –
487 from formation to maturation to maintenance to dispersal. The finding that the loss of different
488 PDEs would result in different phenotypes may be expected given the varied impacts that these
489 enzymes have on the regulation and timing of c-di-GMP signaling and biofilm formation (9, 13).

Here, while we assessed all PDE and dual-domain mutants in *P. aeruginosa* in our initial screen, we only observed consistent and significant defects in biofilm maintenance in the Δ*rmcA* and Δ*morA* mutants. Previous work identified a number of DGCs and PDEs apparently required for early biofilm formation, including SadC, RoeA, BifA, and SiaD (15, 16, 45). In contrast, the PDE DipA has been shown to mediate biofilm dispersion in response to elevated nutrient concentrations and this protein localizes to the cell pole during division, resulting in the asymmetric distribution of c-di-GMP (18, 46). Thus, our data are consistent with the hypothesis of stage-specific roles for DGCs/PDEs in the biofilm life cycle.

The network which controls c-di-GMP levels in *P. aeruginosa* is complex. Identified first in *P. putida,* MorA was found to repress motility in swim assays (37). This same work found that the enhanced motility of the *morA* mutant was not observed in *P. aeruginosa* (37), but previous work from the Hogan and O'Toole labs showed that the Δ*morA* mutant exhibited a significant decrease in flagella-dependent swimming and swarming motility (24). The basis of this difference in phenotypes may be due to the fact that different species of *Pseudomonas* were used in the two studies. Nevertheless, given the role of motility in early biofilm formation, the observation that MorA contributes to swimming and swarming motility indicates that this PDE also likely contributes to the initiation of biofilm communities.

Insightful work from the Dietrich lab provided evidence that RmcA is activated by phenazine availability to mediate a decrease in c-di-GMP levels during oxidative stress conditions (25). In this model, RmcA can act as a redox sensor and may behave as a switch to translate this signal into decreased levels of c-di-GMP and EPS. This model for the role of RmcA in the context of the colony biofilm used by Okegbe, Dietrich and colleagues (25) is largely in agreement with the experimental evidence we have provided, which suggests that RmcA is important for biofilm maintenance. Specifically, it is likely that in mature biofilms with elevated biomass, nutrient

limitation coincides with oxygen depletion and the production and utilization of phenazines as electron shuttles. Indeed, the direct regulatory signal sensed by RmcA appears to be a change in redox state that is likely secondary to the loss of a catabolizable carbon source (25). Thus, in this environment, we hypothesize that RmcA downregulates the production of energetically-expensive Pel EPS, and that failure to do so could result in the observed cell death and biofilm maintenance defect. Together, these data suggest that further examination of these enzymes will generate a more nuanced view of the model presented in **Figure 6**, wherein specific c-di-GMP metabolizing enzymes work at one or more stages of the biofilm life cycle, with the potential to perform several overlapping functions across these various stages (i.e., biofilm initiation and biofilm maintenance).

Materials and Methods

Strains and media. Strains, plasmids and primers used in this study are listed in supplemental Tables S1 and S2. *P. aeruginosa* strain UCBPP-PA14 (PA14) was used in all the experiments, except for the IP studies and the proteins used in the BATCH, which used the PAO1 strains. *P. aeruginosa* were routinely streaked onto lysogeny broth (LB) plates containing 1.5% agar prior to overnight culturing in LB liquid cultures at 37°C. When appropriate, LB was supplemented with 10 µg/ml gentamicin (Gm) and 50 µg/ml kanamycin (Kan). Biofilm medium used in static 96 well crystal violet assays was composed of M63 medium supplemented with 1 mM $MgSO_4$ and 0.4% (w/v) L-arginine monochloride, and where indicated the arginine was replaced by 20 mM pyruvate (3, 47). ALI and microfluidic-based biofilm assays were performed in KA medium, a modification of the previously reported K10T medium (48) containing 50 mM Tris-HCl (pH 7.4), 0.61 mM $MgSO_4$ and 0.4% arginine.

Static biofilm assays and quantification. Overnight cultures were inoculated into 96-well U-bottom polystyrene plates (Costar) containing M63-based medium and grown for the specified time at 37°C in a hydrated container prior to washing, staining with crystal violet, and then solubilization of the crystal violet stain with 30% glacial acetic acid (3, 47). Biofilm was quantified by measuring the extent of biofilm-associated CV solubilized in a spectrophotometer at OD_{550}.

For biofilms imaged microscopically along the ALI, overnight cultures were prepared as described above and inoculated into 12-well dishes containing KA biofilm medium. Glass coverslips were partially submerged in the medium and grown at 37°C for the desired length of time prior to removal and imaging with a Nikon Eclipse Ti inverted microscope where a minimum of ten fields of view were captured. To assess viability of coverslip-grown biofilms, propidium iodide and Syto9 (Molecular Probes® Live/Dead BacLightTM) were gently mixed into the growth medium and biofilms were stained for one hour prior to imaging. Pel was visualized

within the ALI with the addition of 10 µl/ml of Pel-specific fluorescein-labelled *Wisteria floribunda* lectin (Vector Laboratories) to the KA medium at the start of the assay. To assess the concentration of c-di-GMP we utilized the P_{cdrA}-*gfp* fusion expressed from a multicopy pMQ72 (49) which was maintained in overnight cultures supplemented with Gm prior to inoculation into antibiotic-free KA.

Congo Red assay. Strains were grown overnight in 5 ml LB at 37°C and 5 µl of an overnight culture was spotted onto plates containing 1.5% agar, 1% Tryptone, 40 µg/mL Congo Red (CR) and 15 µg/mL Coomassie brilliant blue. The plates were incubated at 37°C for 24 h and imaged after an additional 4 days at room temperature.

Microfluidics. Biofilms were visualized under flow in microfluidics chambers kindly provided by the Nadell laboratory. Chambers used poly-dimethylsiloxane (PDMS) bonded to a 1.5 X 36mm X 60mm cover glass (ThermoFisher, Waltham MA) through soft lithography techniques (50, 51). Overnight bacterial cultures were centrifuged, resuspended in KA, adjusted to an OD_{600} of 1, pipetted into microfluidics chambers and allowed to attach for 1h. Tubing (#30 Cole Palmer PTFE) to transport influent and effluent medium was attached first to BD 5-ml syringes containing KA biofilm medium, then to the microfluidics chambers and then to syringe pumps (Pico Plus Elite, Harvard Apparatus) operating at a flow rate of 0.5 µl/min.

Image acquisition and data analysis. All microscopy was acquired using Nikon Elements AR running a Nikon Eclipse Ti inverted microscope equipped with a Hamamatsu ORCA-Flash 4.0 camera and imaged through either a Plan Apochromat 100x DM Oil or Plan Fluor 40x DIC M N2 objective. Fast scan mode and 2X2 binning was used for imaging. All images were collected in a temperature controlled environmental chamber set to 37°C. Images were processed with background subtraction and signal strength quantified by measuring mean signal intensity/pixel through the Integrated Density (IntDen) function.

574 **Statistical analysis.** Data was analyzed with Graph Pad Prism 8. Unless otherwise noted, data
575 are representative of the results from at least three independent experiments. A Student's *t* test
576 was used to compare results and to assess significance.

577 **Strain construction of fluorescent strains.** *P. aeruginosa* expressing fluorescent GFP were
578 made through electroporation of a multi-copy plasmid pSMC21. mKO was introduced in single
579 copy on the chromosome at the *att*:Tn*7* site via conjugation from *E. coli* S17-λpir pCN768 (52).
580 In-frame, unmarked *rmcA* and *morA* gene deletions were generated using allelic replacement,
581 as reported (53). Construction of gene deletion alleles was performed by amplifying flanking
582 regions of the *rmcA* and *morA* ORFs and joining these flanking regions by splicing-by-overlap
583 extension PCR. The upstream forward and downstream reverse primers were tailed with
584 restriction endonuclease cleavage sequences to enable ligation-dependent cloning of the
585 spliced PCR products. The assembled Δ*rmcA* and Δ*morA* alleles were ligated into pEX18Gm
586 (54) and the resultant allelic exchange vectors were transformed into *E. coli* DH5α. Plasmids
587 were then isolated from individual colonies and verified by Sanger sequencing using M13F and
588 M13R. Plasmids were conjugated into *P. aeruginosa* PA14 from E. coli and merodiploids
589 selected on LB agar containing 10 µg/mL gentamicin. SacB-mediated counter selection was
590 carried out to select for double crossover mutations on no salt LB (NSLB) agar containing 15%
591 (w/v) sucrose. Unmarked gene deletions were identified by colony PCR using primers that
592 targeted the outside, flanking regions of the *rmcA* and *morA* ORFs. These PCR products were
593 Sanger sequenced using the same primers to confirm the correct deletion.
594
595 The Δ*rmcA* and Δ*morA* deletion alleles were introduced into *P. aeruginosa* PAO1 Δ*wspF* Δ*psl*
596 P_{BAD}*pel* (38) via biparental mating with the donor strain *E. coli* SM10 (55). Merodiploids were
597 selected on Vogel-Bonner minimal medium (VBMM) agar containing 30 µg/mL gentamicin.
598 SacB-mediated counter selection was performed to select for double crossover mutations on no

599 salt LB (NSLB) agar containing 15% (w/v) sucrose. Unmarked gene deletions were identified by
600 colony PCR using primers that targeted the outside, flanking regions of the *rmcA* and *morA*
601 ORFs. These PCR products were Sanger sequenced using the same primers to confirm the
602 correct deletion.
603
604 For gene complementation in *P. aeruginosa*, pUC18T-miniTn7T-Gm, which allows for single-
605 copy chromosomal insertion of genes (56), was modified to allow for arabinose-dependent
606 expression of complementing genes. The *araC*-P_{BAD} promoter from pJJH187 (57) was amplified
607 using the primer pair miniTn7-pBAD-F and miniTn7-pBAD-R, the latter of which contains
608 flanking sequence encoding *Sma*I, *Not*I, *Pst*I, and *Nco*I sites to generate a multiple cloning site
609 downstream of the *araC*-P_{BAD} promoter. The resulting PCR product was cloned into the *Sac*I
610 and *Hin*dIII sites of pUC18T-miniTn7T-Gm to generate pUC18T-miniTn7T-Gm-pBAD.
611
612 The ORF corresponding to *rmcA* or *morA* was amplified using primer pairs tailed with restriction
613 endonuclease cleavage sequences to enable ligation-dependent cloning of the PCR products.
614 Upstream primers were also tailed with a synthetic ribosome binding site upstream of the start
615 codon. PCR products were ligated into pUC18T-miniTn7T-Gm-pBAD and the resulting miniTn*7*
616 vectors were transformed into *E. coli* DH5α and selected on LB agar containing 10 µg/mL
617 gentamicin and 100 µg/mL carbenicillin. Plasmids were then isolated from individual colonies
618 and verified by Sanger sequencing using the miniTn7-SEQ-F and miniTn7-SEQ-R primers, as
619 well as primers specific to internal portions of each gene, as appropriate.
620
621 Incorporation of C-terminal vesicular stomatitis virus glycoprotein (VSV-G) tags into p-miniTn7-
622 *rmcA* and p-miniTn7-*morA* was performed via PCR with 5'-phosphorylated primer pairs. The
623 forward primer annealed to the stop codon of *rmcA* or *morA* plus 15-22 bp of downstream vector
624 encoded sequence. The reverse primer annealed to the coding strand 19-21 bp upstream of the

rmcA or *morA* stop codon. The forward and reverse primers contained 5'-overhangs that encoded the last and first halves, respectively, of the VSV-G peptide sequence. The PCR amplified product of these primer pairs was subsequently digested with *Dpn*I for 1 h at 37 °C to remove template DNA, followed by incubation with T4 DNA ligase overnight at room temperature to self-ligate the blunt ends and re-circularize the vector. The resulting C-terminally VSV-G-tagged miniTn7 vectors were transformed into *E. coli* DH5α and selected on LB agar containing 10 µg/mL gentamicin and 100 µg/mL carbenicillin. Plasmids were then isolated from individual colonies and verified by Sanger sequencing as described above.

Complemented *P. aeruginosa* strains were generated through incorporation of miniTn7 vectors at the neutral *att::*Tn*7* site on the *P. aeruginosa* chromosome via electroporation of miniTn7 vectors, along with the helper plasmid pTNS2, as previously described (56). Transposon mutants were selected on LB agar containing 30 µg/mL gentamicin.

Co-immunoprecipitation assays. 1 L of LB, containing 0.5% (w/v) L-arabinose and 30 µg/mL gentamicin, was inoculated with a *P. aeruginosa* strain carrying a VSV-G-tagged protein and allowed to grow overnight at 37 °C with shaking at 200 RPM. The next day, cells were collected at 5,000 × *g* for 20 min at 4 °C. Cell pellets were resuspended in 5 mL of 0.2 M Tris-HCl pH 8, 1 M sucrose, 1 mM EDTA, and 1 mg/mL lysozyme. Cells were incubated for 10 min at room temperature prior to the addition of 20 mL of water and further incubation on ice for 30 min. The resultant solution was centrifuged at 30,000 × *g* for 20 min at 4 °C to collect spheroplasts. The pellet was then resuspended in 50 mL of 10 mM Tris-HCl pH 7.5, 5 mM EDTA, and 1 mM DTT, and lysed by homogenization using an Emulsiflex-C3 (Avestin Inc.) at a pressure of 10,000 - 15,000 psi until the solution appeared translucent. The solution was clarified by centrifugation at 30,000 × *g* for 20 min at 4 °C, and the resultant supernatant was further centrifuged at 180,000 × *g* for 1 h at 4 °C to collect the membranes. Membranes were then solubilized in 10 mL of

651 Buffer A (50 mM Tris-HCl pH 8, 10 mM $MgCl_2$, and 2% (w/v) Triton X-100) using a Dounce
652 homogenizer and centrifuged at 90,000 × *g* for 30 min at 4 °C to clarify the solution. A sample of
653 the solubilized membranes was collected before application to the IP resin as a representative
654 example of the input into the experiment. The IP resin (Sigma anti-VSV-G monoclonal antibody-
655 agarose conjugate) was prepared by mixing 60 µL of resin slurry with 10 mL of Buffer A,
656 followed by collection of the IP resin by centrifugation at 100 × *g* for 2 min at 4 °C and removal
657 of the supernatant. The solubilized membranes were applied to the washed IP resin and
658 incubated at 4 °C for 1 h with agitation. The IP resin was then collected by centrifugation at 100
659 × *g* for 2 min at 4 °C and the supernatant discarded. The resin was washed five times with 10
660 mL of Buffer A as above to remove non-specifically bound protein. The resin was then mixed
661 with 150 µL of 2× Laemmli buffer, boiled at 95 °C for 10 min, and analyzed by SDS-PAGE
662 followed by Western blotting as described below. As a negative control, the above experimental
663 protocol was also performed using a *P. aeruginosa* strain carrying the corresponding untagged
664 protein.
665
666 **Western blot sample analysis**. For Western blots, a 0.2 µm PVDF membrane was wetted in
667 methanol and soaked for 5 min in Western transfer buffer (25 mM Tris-HCl, 150 mM glycine,
668 20% (v/v) methanol) along with the SDS-PAGE gel to be analyzed. Protein was transferred from
669 the SDS-PAGE gel to the PVDF membrane by wet blotting (25 mV, 2 h). The membrane was
670 briefly washed in Tris-buffered saline (10 mM Tris-HCl pH 7.5, 150 mM NaCl) containing 0.5%
671 (v/v) Tween-20 (TBS-T) before blocking in 5% (w/v) skim milk powder in TBS-T for 2 h at room
672 temperature with gentle agitation. The membrane was briefly washed again in TBS-T before
673 incubation overnight with primary antibody (1:5000 α-PelD polyclonal antibody (36) or 1:75000
674 Sigma α-VSV-G monoclonal antibody) in TBS-T with 1% (w/v) skim milk powder at 4 °C. The
675 next day, the membrane was washed four times in TBS-T for 5 min each before incubation for 1
676 h with secondary antibody (1:2000 dilution of BioRad affinity purified goat α-rabbit or goat α-

677 mouse IgG conjugated to alkaline phosphatase) in TBS-T with 1% (w/v) skim milk powder. The
678 membrane was then washed four times with TBS-T for 5 min each before development with 5-
679 bromo-4-chloro-3-indolyl phosphate/nitro blue tetrazolium chloride (BioShop ready-to-use
680 BCIP/NBT solution). Developed blots were imaged using a BioRad ChemiDoc imaging system.
681
682 **Bacterial adenylate cyclase two-hybrid (BACTH) assays**. Cloning of *rmcA* and *morA* into the
683 BACTH assay-compatible vector pUT18C, and *pelD* into pKT25, was performed using standard
684 molecular methods. Reverse primers were flanked with a 3'-stop codon for cloning into pUT18C
685 and pKT25, which encode a N-terminal adenylate cyclase fragment fusion (39). Primer pairs
686 were tailed with restriction endonuclease cleavage sequences to enable ligation-dependent
687 cloning and were used to amplify the corresponding *pelD*, *rmcA*, and *morA* genes from PAO1
688 genomic DNA. PCR products were digested with the appropriate restriction endonucleases and
689 ligated into pUT18C and pKT25, as appropriate. Ligations were transformed into *E. coli* DH5α
690 and selected on LB agar containing 50 µg/mL kanamycin for pKT25 clones, or 100 µg/mL
691 carbenicillin for pUT18C clones. Plasmids were then isolated from individual colonies and
692 verified by Sanger sequencing using primers specific for pUT18C and pKT25, as well as primers
693 specific to internal segments of *rmcA* and *morA*, as appropriate. Positive clones were verified as
694 above.
695
696 Combinations of the above T18 and T25 fusion proteins were transformed into the BACTH
697 compatible strain BTH101 (Euromedex) for analysis. For each experiment, 5 mL of LB
698 supplemented with 50 µg/mL kanamycin, 100 µg/mL carbenicillin, and 0.5 mM IPTG was
699 inoculated with the appropriate BTH101 strain and grown overnight at 30 °C with shaking at 200
700 RPM. The next day, 2 µL of culture was used to spot inoculate a LB agar plate containing 50
701 µg/mL kanamycin, 100 µg/mL carbenicillin, 0.5 mM IPTG, and 50 µg/mL 5-bromo-4-chloro-3-
702 indolyl-β-D-galactopyranoside (X-Gal). The plates were incubated for 24 h at 30 °C and

703 subsequently photographed. The vectors pUT18C::zip and pKT25::zip (39) were used as a
704 positive control. Empty pUT18C and pKT25 vectors were used as a negative control.
705
706 To generate tag-free expression constructs for the modified BACTH assays, *pelE* and *pelG*
707 were amplified from PAO1 genomic DNA using forward primers that were flanked with a
708 synthetic ribosome binding site and reverse primers flanked with a 3'-stop codon. PCR products
709 were subsequently digested with *Eco*RI and *Hin*dIII and ligated into the arabinose-inducible
710 expression vector pBADGr (10 Clones with positive inserts were verified by Sanger sequencing
711 using the BADGr-SEQ-F and BADGr-SEQ-R primers). The vector expressing both *pelE* and
712 *pelG* was generated by amplifying the *pelE* and *pelG* ORFs from *P. aeruginosa* genomic DNA.
713 The intervening *pelF* ORF from the *pel* operon was excluded by joining the upstream *pelE* and
714 downstream *pelG* ORFs via the splicing-by-overlap extension PCR method, as described above
715 for generation of chromosomal deletion alleles, to generate a single polycistronic strand. All
716 assays with untagged constructs were performed as above, with the addition of 10 µg/mL
717 gentamicin and 0.5% (w/v) arabinose to all growth media for, respectively, maintenance of and
718 expression from pBADGr. Empty pBADGr was used as a vector control.
719
720 **Acknowledgements**. We thank C. Nadell for providing the fluorescent protein constructs and
721 help with preparing the microfluidic chambers. We thank A. Collins and G. Heussler for the
722 constructive feedback throughout the course of this research. This work was supported by NIH
723 Grant R37 AI83256-06 to G.A.O and the Canadian Institutes of Health Research (CIHR) MOP
724 43998 and FDN154327 to PLH. PLH is the recipient of a Tier I Canada Research Chair. GBW
725 was supported in part by a Canada Graduate Scholarship from the Natural Sciences and
726 Engineering Research Council of Canada (NSERC) and a graduate scholarship from Cystic
727 Fibrosis Canada.

728 **References.**

729 1. Sauer K, Camper AK, Ehrlich GD, Costerton JW, Davies DG. 2002. *Pseudomonas*
730 *aeruginosa* displays multiple phenotypes during development as a biofilm. Journal of
731 Bacteriology 184:1140–1154.
732 2. Toutain CM, Caizza NC, Zegans ME, O'Toole GA. 2007. Roles for flagellar stators in
733 biofilm formation by *Pseudomonas aeruginosa*. Research in Microbiology 158:471–477.
734 3. O'Toole GA, Kolter R. 1998. Flagellar and twitching motility are necessary for
735 *Pseudomonas aeruginosa* biofilm development. Molecular Microbiology 30:295–304.
736 4. Ghafoor A, Hay ID, Rehm BHA. 2011. Role of exopolysaccharides in *Pseudomonas*
737 *aeruginosa* biofilm formation and architecture. Applied and Environmental Microbiology
738 77:5238–5246.
739 5. Colvin KM, Gordon VD, Murakami K, Borlee BR, Wozniak DJ, Wong GCL, Parsek MR.
740 2011. The Pel polysaccharide can serve a structural and protective role in the biofilm
741 matrix of *Pseudomonas aeruginosa*. PLoS Pathogens 7:e1001264.
742 6. Flemming HC, Wingender J. 2001. Relevance of microbial extracellular polymeric
743 substances (EPSs) - Part I: Structural and ecological aspects. Water Science and
744 Technology 43:1–8.
745 7. Jenal U, Reinders A, Lori C. 2017. Cyclic di-GMP: Second messenger extraordinaire.
746 Nature Reviews Microbiology 15:271–284.
747 8. Simm R, Morr M, Kader A, Nimtz M, Römling U. 2004. GGDEF and EAL domains
748 inversely regulate cyclic di-GMP levels and transition from sessibility to motility. Molecular
749 Microbiology 53:1123–1134.
750 9. Valentini M, Filloux A. 2019. Multiple roles of c-di-GMP signaling in bacterial
751 pathogenesis. Annual Review of Microbiology 73:387–406.
752 10. Hickman JW, Harwood CS. 2008. Identification of FleQ from *Pseudomonas aeruginosa*
753 as a c-di-GMP-responsive transcription factor. Molecular Microbiology 69:376–389.

754 11. Ryan RP, Fouhy Y, Lucey JF, Crossman LC, Spiro S, He YW, Zhang LH, Heeb S,
755 Cámara M, Williams P, Dow JM. 2006. Cell-cell signaling in *Xanthomonas campestris*
756 involves an HD-GYP domain protein that functions in cyclic di-GMP turnover.
757 Proceedings of the National Academy of Sciences of the United States of America
758 103:6712–6717.
759 12. Kulesekara H, Lee V, Brencic A, Liberati N, Urbach J, Miyata S, Lee DG, Neely AN,
760 Hyodo M, Hayakawa Y, Ausubel FM, Lory S. 2006. Analysis of *Pseudomonas aeruginosa*
761 diguanylate cyclases and phosphodiesterases reveals a role for bis-(3′-5′)-cyclic-GMP in
762 virulence. Proceedings of the National Academy of Sciences of the United States of
763 America 103:2839–2844.
764 13. Ha D-G, O'Toole GA. 2015. c-di-GMP and its effects on biofilm formation and dispersion:
765 a *Pseudomonas aeruginosa* review. Microbiology Spectrum 3:1–12.
766 14. Romling U, Galperin MY, Gomelsky M. 2013. Cyclic di-GMP: the first 25 years of a
767 universal bacterial second messenger. Microbiology and Molecular Biology Reviews
768 77:1–52.
769 15. Merritt JH, Brothers KM, Kuchma SL, O'Toole GA. 2007. SadC reciprocally influences
770 biofilm formation and swarming motility via modulation of exopolysaccharide production
771 and flagellar function. Journal of Bacteriology 189:8154–8164.
772 16. Kuchma SL, Brothers KM, Merritt JH, Liberati NT, Ausubel FM, O'Toole GA. 2007. BifA, a
773 cyclic-di-GMP phosphodiesterase, inversely regulates biofilm formation and swarming
774 motility by *Pseudomonas aeruginosa* PA14. Journal of Bacteriology 189:8165–8178.
775 17. Hickman JW, Tifrea DF, Harwood CS. 2005. A chemosensory system that regulates
776 biofilm formation through modulation of cyclic diguanylate levels. Proceedings of the
777 National Academy of Sciences of the United States of America 102:14422–14427.
778 18. Roy AB, Petrova OE, Sauer K. 2012. The phosphodiesterase DipA (PA5017) is essential
779 for *Pseudomonas aeruginosa* biofilm dispersion. Journal of Bacteriology 194:2904–2915.

780 19. Li Y, Heine S, Entian M, Sauer K, Frankenberg-Dinkel N. 2013. NO-induced biofilm
781 dispersion in *Pseudomonas aeruginosa* is mediated by an MHYT domain-coupled
782 phosphodiesterase. Journal of Bacteriology 195:3531–3542.
783 20. Southey-Pillig CJ, Davies DG, Sauer K. 2005. Characterization of temporal protein
784 production in *Pseudomonas aeruginosa* biofilms. Journal of Bacteriology 187:8114–8126.
785 21. Heussler GE, Cady KC, Koeppen K, Bhuju S, Stanton BA, O'Toole GA. 2015. Clustered
786 regularly interspaced short palindromic repeat-dependent, biofilm-specific death of
787 pseudomonas aeruginosa mediated by increased expression of phage-related genes.
788 mBio 6:1–13.
789 22. Dahlstrom KM, Giglio KM, Sondermann H, O'Toolea GA. 2016. The inhibitory site of a
790 diguanylate cyclase is a necessary element for interaction and signaling with an effector
791 protein. Journal of Bacteriology 198:1595–1603.
792 23. Schultz J, Milpetz F, Bork P, Ponting CP. 1998. SMART, a simple modular architecture
793 research tool: Identification of signaling domains. Proceedings of the National Academy
794 of Sciences of the United States of America 95:5857–5864.
795 24. Ha DG, Richman ME, O'Toole GA. 2014. Deletion mutant library for investigation of
796 functional outputs of cyclic diguanylate metabolism in *Pseudomonas aeruginosa* PA14.
797 Applied and Environmental Microbiology 80:3384–3393.
798 25. Okegbe C, Fields BL, Cole SJ, Beierschmitt C, Morgan CJ, Price-Whelan A, Stewart RC,
799 Lee VT, Dietrich LEP. 2017. Electron-shuttling antibiotics structure bacterial communities
800 by modulating cellular levels of c-di-GMP. Proceedings of the National Academy of
801 Sciences of the United States of America 114:E5236–E5245.
802 26. Phippen CW, Mikolajek H, Schlaefli HG, Keevil CW, Webb JS, Tews I. 2014. Formation
803 and dimerization of the phosphodiesterase active site of the *Pseudomonas aeruginosa*
804 MorA, a bi-functional c-di-GMP regulator. FEBS Letters 588:4631–4636.
805 27. Rybtke MT, Borlee BR, Murakami K, Irie Y, Hentzer M, Nielsen TE, Givskov M, Parsek

MR, Tolker-Nielsen T. 2012. Fluorescence-based reporter for gauging cyclic di-GMP levels in *Pseudomonas aeruginosa*. Applied and Environmental Microbiology 78:5060–5069.

28. Karasawa S, Araki T, Nagai T, Mizuno H, Miyawaki A. 2004. Cyan-emitting and orange-emitting fluorescent proteins as a donor/acceptor pair for fluorescence resonance energy transfer. Biochemical Journal 381:307–312.

29. Merritt JH, Kadouri DE, O'Toole GA. 2005. Growing and analyzing static biofilms. current protocols in microbiology 22:1–17.

30. Kolter R, Bloemberg G V, O'Toole G, Lugtenberg BJ. 1997. Green fluorescent protein as a marker for *Pseudomonas* spp. Applied and Environmental Microbiology 63:4543-4551.

31. Mah TF, Pitts B, Pellock B, Walker GC, Stewart PS, O'Toole GA. 2003. A genetic basis for *Pseudomonas aeruginosa* biofilm antibiotic resistance. Nature 426:306–310.

32. Jennings LK, Storek KM, Ledvina HE, Coulon C, Marmont LS, Sadovskaya I, Secor PR, Tseng BS, Scian M, Filloux A, Wozniak DJ, Howell PL, Parsek MR. 2015. Pel is a cationic exopolysaccharide that cross-links extracellular DNA in the *Pseudomonas aeruginosa* biofilm matrix. Proceedings of the National Academy of Sciences of the United States of America 112:11353–11358.

33. Baraquet C, Murakami K, Parsek MR, Harwood CS. 2012. The FleQ protein from *Pseudomonas aeruginosa* functions as both a repressor and an activator to control gene expression from the Pel operon promoter in response to c-di-GMP. Nucleic Acids Research 40:7207–7218.

34. Lee VT, Matewish JM, Kessler JL, Hyodo M, Hayakawa Y, Lory S. 2007. A cyclic-di-GMP receptor required for bacterial exopolysaccharide production. Molecular Microbiology 65:1474–1484.

35. Dahlstrom KM, O'Toole GA. 2017. A symphony of cyclases: Specificity in diguanylate cyclase signaling. Annual Review of Microbiology 71:179–195.

832 36. Whitfield GB, Marmont LS, Ostaszewski A, Rich JD, Whitney JC, Parsek MR, Harrison
833 JJ, Howell PL. 2020. Pel polysaccharide biosynthesis requires an inner membrane
834 complex comprised of PelD, PelE, PelF, and PelG. Journal of bacteriology 202:e00684-
835 19.
836 37. Choy WK, Zhou L, Syn CKC, Zhang LH, Swarup S. 2004. MorA defines a new class of
837 regulators affecting flagellar development and biofilm formation in diverse *Pseudomonas*
838 *species*. Journal of Bacteriology 186:7221–7228.
839 38. Colvin KM, Alnabelseya N, Baker P, Whitney JC, Lynne Howell P, Parsek MR. 2013.
840 PelA deacetylase activity is required for pel polysaccharide synthesis in *Pseudomonas*
841 *aeruginosa*. Journal of Bacteriology 195:2329–2339.
842 39. Karimova G, Ullmann A, Ladant D. 2001. Protein-protein interaction between *Bacillus*
843 *stearothermophilus* tyrosyl-tRNA synthetase subdomains revealed by a bacterial two-
844 hybrid system. Journal of Molecular Microbiology and Biotechnology 3:73–82.
845 40. Díaz-Salazar C, Calero P, Espinosa-Portero R, Jiménez-Fernández A, Wirebrand L,
846 Velasco-Domínguez MG, López-Sánchez A, Shingler V, Govantes F. 2017. The stringent
847 response promotes biofilm dispersal in *Pseudomonas putida*. Scientific Reports 7:1–13.
848 41. Jimenez-Fernandez A, Lopez-Sanchez A, Calero P, Govantes F. 2015. The c-di-GMP
849 phosphodiesterase BifA regulates biofilm development in *Pseudomonas putida*.
850 Environmental Microbiology Reports 7:78–84.
851 42. Friedman L, Kolter R. 2004. Genes involved in matrix formation in *Pseudomonas*
852 *aeruginosa* PA14 biofilms. Molecular Microbiology 51:675–690.
853 43. Bernier SP, Ha DG, Khan W, Merritt JH, O'Toole GA. 2011. Modulation of *Pseudomonas*
854 *aeruginosa* surface-associated group behaviors by individual amino acids through c-di-
855 GMP signaling. Research in Microbiology 162:680–688.
856 44. Lin YC, Cornell WC, Jo J, Price-Whelan A, Dietrich LEP. 2018. The *Pseudomonas*
857 *aeruginosa* complement of lactate dehydrogenases enables use of d -and l -lactate and

858 metabolic cross-feeding. mBio 9:1–12.

859 45. Klebensberger J, Birkenmaier A, Geffers R, Kjelleberg S, Philipp B. 2009. SiaA and SiaD
860 are essential for inducing autoaggregation as a specific response to detergent stress in
861 *Pseudomonas aeruginosa*. Environmental Microbiology 11:3073–3086.

862 46. Kulasekara BR, Kamischke C, Kulasekara HD, Christen M, Wiggins PA, Miller SI. 2013.
863 c-di-GMP heterogeneity is generated by the chemotaxis machinery to regulate flagellar
864 motility. eLife 2013:1–19.

865 47. Cady KC, O'Toole GA. 2011. Non-identity-mediated CRISPR-bacteriophage interaction
866 mediated via the Csy and Cas3 proteins. Journal of Bacteriology 193:3433–3445.

867 48. Monds RD, Newell PD, Schwartzman JA. 2006. Conservation of the Pho regulon in.
868 Society 72:1910–1924.

869 49. Shanks RMQ, Caiazza NC, Hinsa SM, Toutain CM, O'Toole GA. 2006. *Saccharomyces*
870 *cerevisiae*-based molecular tool kit for manipulation of genes from gram-negative
871 bacteria. Applied and Environmental Microbiology 72:5027–5036.

872 50. Sia SK, Whitesides GM. 2003. Microfluidic devices fabricated in poly(dimethylsiloxane)
873 for biological studies. Electrophoresis 24:3563–3576.

874 51. Weibel DB, DiLuzio WR, Whitesides GM. 2007. Microfabrication meets microbiology.
875 Nature Reviews Microbiology 5:209–218.

876 52. Wucher BR, Bartlett TM, Hoyos M, Papenfort K, Persat A, Nadell CD. 2019. *Vibrio*
877 *cholerae* filamentation promotes chitin surface attachment at the expense of competition
878 in biofilms. Proceedings of the National Academy of Sciences of the United States of
879 America 116:14216–14221.

880 53. Hmelo LR, Borlee BR, Almblad H, Love ME, Randall TE, Tseng BS, Lin C, Irie Y, Storek
881 KM, Yang JJ, Siehnel RJ, Howell PL, Singh PK, Tolker-Nielsen T, Parsek MR, Schweizer
882 HP, Harrison JJ. 2015. Precision-engineering the *Pseudomonas aeruginosa* genome with
883 two-step allelic exchange. Nature Protocols 10:1820–1841.

884 54. Hoang TT, Karkhoff-Schweizer RR, Kutchma AJ, Schweizer HP. 1998. A broad-host-
885 range F1p-FRT recombination system for site-specific excision of chromosomally-located
886 DNA sequences: Application for isolation of unmarked *Pseudomonas aeruginosa*
887 mutants. Gene 212:77–86.
888 55. de Lorenzo V, Timmis KN. 1994. Analysis and construction of stable phenotypes in
889 Gram-negative bacteria with Tn5- and Tn10-derived minitransposons. Methods in
890 Enzymology 235:386–405.
891 56. Choi KH, Gaynor JB, White KG, Lopez C, Bosio CM, Karkhoff-Schweizer RAR,
892 Schweizer HP. 2005. A Tn7-based broad-range bacterial cloning and expression system.
893 Nature Methods 2:443–448.
894 57. Almblad H, Harrison JJ, Rybtke M, Groizeleau J, Givskov M, Parsek MR, Tolker-Nielsen
895 T. 2015. The cyclic AMP-Vfr signaling pathway in *Pseudomonas aeruginosa* is inhibited
896 by cyclic Di-GMP. Journal of Bacteriology 197:2190–2200.
897

898 **Figure legends**

899

900 **Figure 1. CRISPR-activated *P. aeruginosa* is unable to maintain a biofilm but can be**
901 **rescued by modulating c-di-GMP levels**. (A) Biofilm assays were performed as detailed in
902 Materials and Methods and grown in M63 medium supplemented with 0.4% L-arginine, which
903 we refer to as the "biofilm medium" in the text. WT (*P. aeruginosa* PA14) and the strain carrying
904 the DMS3$_{42}$ insertion at the *att* site (*att*::DMS3$_{42}$), carrying either the empty vector (EV) or a
905 plasmid expressing the constitutively-active diguanylate cyclase GcbC-R363E, were grown
906 statically for 12 h then biofilm formation assessed. The OD$_{550}$ value represents a measure of the
907 biofilm formed. Error bars represent standard deviation of the results from three biological
908 replicates each performed with three technical replicates. *** indicates a difference in biofilm
909 levels that is significantly different at a P value of <0.001 for the indicated strains. (B) Previous
910 work by Ha and colleagues (24) created in-frame, unmarked deletions of all putative
911 phosphodiesterases that were identified via SMART analyses of the *P. aeruginosa* genome.
912 The deletion constructs were introduced into the *att*::DMS3$_{42}$ background, and mutations in two
913 genes indicated by red stars, *rmcA* (Δ*rmcA att*::DMS3$_{42}$) and Δ*morA* (Δ*morA att*::DMS3$_{42}$) were
914 found to produce significantly more biofilm compared to the *att*::DMS3$_{42}$ strain. (C) The Δ*rmcA*
915 and Δ*morA* mutations in the WT or the CRISPR-activated background (*att*::DMS3$_{42}$) were
916 assessed for biofilm formation after 12h. The OD$_{550}$ value represents a measure of the biofilm
917 formed. Error bars represent standard deviation of the results from three biological replicates
918 each performed with three technical replicates. **** indicates a difference in biofilm levels that is
919 significantly different at a P value <0.0001 compared to the respective WT *att*::DMS3$_{42}$ strain.

920

921 **Figure 2. The Δ*rmcA* and Δ*morA* mutants are defective in biofilm maintenance and show**
922 **increased levels of c-di-GMP.** (A) The WT strain (*P. aeruginosa* PA14) and the Δ*rmcA* and
923 Δ*morA* mutant strains were grown statically in a 96 well dish assay using M63 medium

924 supplemented with 0.4% L-arginine, and the biofilm formed measured at the indicated
925 timepoints. *** indicates a difference in biofilm that is significantly different at a P value of
926 <0.001 at the indicated time point and each subsequent time point. (B) The WT, Δ*rmcA* mutant,
927 and the Δ*rmcA*::*rmcA*$^{+}$ complemented strain were grown for 48 h prior to crystal violet staining
928 to assess the extent of biofilm formation. *** indicates a difference that is significantly different
929 at a P value of <0.01 compared to the WT; ns is not significant. (C) The WT, Δ*morA* mutant, and
930 the Δ*morA*::*morA*$^{+}$ complemented strain were grown for 48 h prior to crystal violet staining to
931 assess the extent of biofilm formation. *** indicates a difference that is significantly different at a
932 P value of <0.01 compared to the WT. (D) The WT and the Δ*rmcA* and Δ*morA* mutants carrying
933 the P_{cdrA}-*gfp* fusion expressed from a multicopy plasmid were grown along the air-liquid
934 interface of 18 mm glass coverslips and were imaged after 24 hr. Fluorescent microscopy was
935 used to determine GFP signal intensity. (E) Quantification of GFP signal intensity for the strains
936 described in panel D. Fluorescent microscopy was used to determine GFP signal intensity as a
937 measure of c-di-GMP production, which was normalized to constitutively active mKO fluorescent
938 protein. **** indicates a difference in biofilm that is significantly different at a P value < 0.0001
939 compared to the WT strain. In all panels, error bars represent standard deviation from three
940 biological replicates each performed with three technical replicates.
941
942 **Figure 3. The biofilm defect of Δ*rmcA* and Δ*morA* mutants coincides with cell death.** The
943 WT strain (*P. aeruginosa* PA14) and the Δ*rmcA* and Δ*morA* mutants were grown along the air-
944 liquid interface of 18 mm glass coverslips. At 24 h the coverslips were removed, washed in PBS
945 and stained with Syto-9 and propidium iodide (PI). Fluorescent microscopy was used to
946 measure the Syto-9 and PI fluorescence (panel A) and image intensity assessed as a ratio live
947 (Syto-9) to dead (PI) was determined at 16 h (panel B, left) and 48 h (panel B, right). Error bars
948 represent standard deviation from three biological replicates each performed with three
949 technical replicates. *** and **** indicate a difference in biofilm that is significantly different at a

P value of <0.001 and <0.0001, respectively, compared to the WT; ns, not significant. (C) The WT strain and the Δ*rmcA* and Δ*morA* mutants carrying plasmid pSMC21 were grown for 23 h in biofilm medium containing 0.4% L-arginine and stained under flow for an additional 1 h in biofilm medium containing propidium iodide (PI). After this 24 h period of incubation, the biofilm medium was replaced with medium containing PI and lacking arginine; this was considered to be time = 0 h of nutrient limitation (top panel). The biofilms imaged after 36 h of nutrient limitation are shown at the bottom of the panel. (D) GFP fluorescence of the biofilms in panel C were measured every 45 minutes for 36 hrs. WT and the mutants were assessed for changes in GFP fluorescence and plotted as a fraction of GFP signal at the start of nutrient limitation. (E) PI staining of the corresponding biofilms from panel C are shown just prior to nutrient limitation and after 36 h of nutrient limitation. (F) PI straining normalized to GFP fluorescence of pSMC21 is plotted for data acquired in panels C and E every 45 minutes. Error bars represent standard deviation from three biological replicates each performed with three technical replicates. **** indicates a difference in biofilm that is significantly different at a P value of <0.0001, a level of significance observed after 23 h of exposure to nutrient-limited conditions, and at all subsequent time points.

Figure 4. Loss of stringent response phenocopies biofilm defect and cell death observed for the PDE mutants. (A) The WT (*P. aeruginosa* PA14) strain and the Δ*relA*Δ*spoT* double mutant strain were grown statically in a 96 well dish assay using M63 medium supplemented with 0.4% L-arginine, and biofilm formed was measured at the indicated timepoints. (B) The WT strain and the Δ*relA*Δ*spoT* double mutant, both carrying pSMC21, were grown for 23 h using a microfluidic device in biofilm medium containing 0.4% L-arginine and stained under flow for an additional 1 h in biofilm medium containing propidium iodide (PI). The biofilm medium was then replaced with medium containing PI and lacking arginine. The fluorescence due to GFP and PI for the WT strain and the Δ*relA*Δ*spoT* double mutant are shown at the start of nutrient limitation

(0 hr, top) and after 24 h (bottom) in the microfluidic chamber. (C) GFP fluorescence was measured every 45 minutes for 24 h after the initiation of nutrient limitation. The WT strain and the Δ*relA*Δ*spoT* double mutant strain were assessed for changes in GFP fluorescence, which was normalized to the GFP signal at the start of nutrient limitation, which is set to 1. (D) The ratio of PI to GFP during ~25 h of nutrient limitation in the microfluidic chamber is presented as a measure of cell viability, with larger values indicating more cell death. For all panels, error bars represent standard deviation from three biological replicates each performed with three technical replicates. Shown is a representative experiment. **** indicates a difference in biofilm that is significantly different at a P value of <0.0001 at the indicated time point and each subsequent time point.

Figure 5. The loss of RmcA or MorA function results in increased Pel production likely through physical interaction with the Pel complex. (A) Cultures of the indicated *P. aeruginosa* PA14 strains were inoculated into lysogeny broth (LB) and imaged after overnight growth at 37°C. The resulting wall-associated material is indicated by the yellow arrows. (B) Congo Red plate assays of the indicated *P. aeruginosa* PA14 strains are shown. The plates were incubated for 24 h at 37°C then at room temperature for an additional 4 days. (C) The WT (*P. aeruginosa* PA14) strain and the Δ*rmcA* and Δ*morA* mutants were grown as a biofilm in the ALI assay for 18 h in medium containing fluorescein-labeled WGA and washed before imaging by fluorescence microscopy. (D) Quantification of the experiment performed in panel C. The fluorescence attributable to the fluorescein-labeled WGA was normalized to the mKO fluorescent protein expressed from the chromosome of each strain and plotted. Error bars represent standard deviation from three biological replicates each performed with three technical replicates. ** and **** indicate a difference in biofilm that is significantly different at a P value of <0.01 and 0.0001, respectively. (E) Co-IP from solubilized *P. aeruginosa* PAO1 inner membranes expressing VSV-G-tagged RmcA (RmcA-V, *left*) or MorA (MorA-V, *right*) as the

bait. The corresponding untagged proteins (RmcA, MorA) were used as a negative binding control. Proteins applied to the α-VSV-G co-IP resin (in, input) and the elution from the resin after washing (IP, immunoprecipitated) were analyzed by Western blot using VSV-G and PelD specific antibodies, as indicated. (F) Representative colony images for the analysis of interactions between RmcA, fused at the N-terminus to the T18 domain of *Bordetella pertussis* adenylate cyclase toxin (T18-RmcA), and PelD fused to the T25 adenylate cyclase domain at the N-terminus (T25-PelD), by BACTH using solid media containing X-Gal as a reporter. The assay was modified through the additional of an empty vector control (VC) for expression of untagged PelE, untagged PelG, or both PelE and PelG (PelEG). A blue colony indicates a positive result in this assay. Empty vectors expressing the T18 or T25 domain alone (empty) were used as a negative control. Fusion of the T18 and T25 domains to a leucine zipper motif (zip) was used as a positive control. (G) Representative colony images for the analysis of interactions between MorA, fused to the T18 domain at the N-terminus (T18-RmcA), and T25-PelD by BACTH. Experiments were performed as described for panel F. Note: The proteins used in these BATCH assays were derived from *P. aeruginosa* PAO1, which are 99% identical to the *P. aeruginosa* PA14 proteins. (H) A model for the RmcA and MorA proteins in complex with the Pel biosynthetic complex (PelDEFG). 5'-pGpG (diamonds) represents the product of the PDE-mediated degradation of c-di-GMP.

Figure 6. A model for MorA and RmcA-mediated biofilm maintenance. Model for RmcA- and MorA-mediated biofilm maintenance in *P. aeruginosa.* Typical biofilm development (top panel) involves surface attachment, after which increased c-di-GMP and EPS synthesis mediate microcolony development and increased biofilm biomass. During the maturation and maintenance phase of biofilm development, regulatory changes reflect growth in a nutrient-limited environment and result in a decrease in the production of energetically expensive products like Pel, reduced c-di-GMP (cdG) and induction of the stringent response. Loss of

RmcA or MorA (bottom panel) results in enhanced c-di-GMP and Pel production and increased biomass in nutrient rich environments. The Δ*rmcA* and Δ*morA* mutant biofilms are unable to appropriately respond to nutrient limitation, resulting in cell death and loss of biofilm biomass.

List of Supplementary Material.

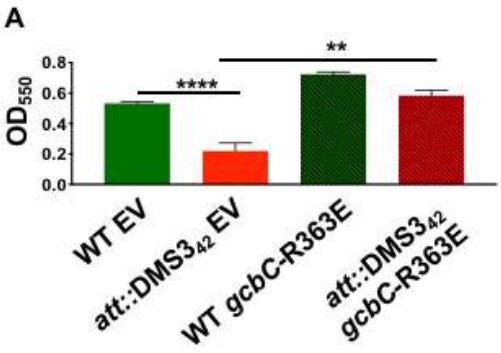

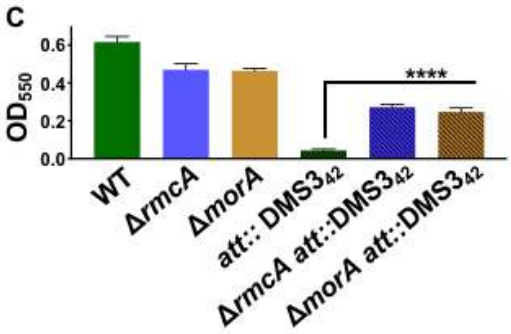

B

	PAO1#	PA14#	
	285	3720	dual domain (GGDEF/EAL)
★	0575 (*rmcA*)	7500	
	3311 (*nbdA*)	21190	
	3258	21870	
	2567	31330	
	2072	37690	
	1727 (*mucR*)	42220	
	1433	45930	
	1181	49160	
	0861 (*rbdA*)	53140	
	4367 (*bifA*)	56790	
★	4601 (*morA*)	60870	
	4959 (*fimX*)	65540	
	5017 (*dipA*)	66320	
	5295	69900	
	5442	71850	EAL
	3947 (*rocR*)	12810	
	3825	14530	
	2200	36260	
	2133	36990	
	NA (*pvrR*)	59790	
	4108	10820	HD-GYP
	2572	30830	
	4781	63210